



Spin Prepolarization with a Compact Superconducting Magnet

Paul Jelden^{1,3}, Magnus Dam¹, Jens Hänisch¹, Martin Börner², Sören Lehmkuhl², Bernhard Holzapfel¹,
Tabea Arndt^{1,3}, and Jan G. Korvink^{2,3}

¹Institute for Technical Physics, Karlsruhe Institute of Technology, Eggenstein-Leopoldshafen, 76344, Germany

²Institute of Microstructure Technology, Karlsruhe Institute of Technology, Eggenstein-Leopoldshafen, 76344, Germany

³Corresponding authors: paul.jelden@partner.kit.edu, tabea.arndt@kit.edu, jan.korvink@kit.edu

Research highlights:

- Compact scalable and cryogen-free high-field magnet provides enhanced spin polarization.
- The polarization magnet's stray field conserves the alignment of spins during rapid, adiabatic transfer.
- Using an external 5 T magnet, the net polarization enhancement for protons, accounting for transfer losses, is 2.6 times that measured in a 1.4 T magnet.
- Recently, higher polarization fields (Hahn et al., 2019) have been reported in the literature, which could yield up to 28 times the SNR of the permanent magnet, thus indicating the tremendous potential of the brute-force approach.

Abstract. Compact benchtop NMR systems provide excellent and affordable access to good-quality NMR spectroscopy. Nevertheless, such systems are limited by low polarization levels, resulting in low signal-to-noise ratios compared to those of high-field systems. We show here that polarization levels can be significantly improved by using a medium-homogeneity high-field magnet as a spin prepolarizer. For this type of brute-force hyperpolarization we employ a cryogen-free 5 T superconducting magnet. Because such systems typically lack shielding and thus have noticeable stray fields, samples can be transferred adiabatically from the prepolarizer to the bore of a commercial benchtop NMR system. By adjusting the physical separation between the two magnets, and hence ensuring a sufficiently strong stray field during sample transfer, we report a ¹H polarization enhancement of up to a factor of 2.62 as a first demonstration of the utility. By employing 2G-HTS magnets, higher magnetic fields would become possible while minimizing the size and stray field of the magnet, so that the polarization levels can be further increased in a foreseeable future with moderate effort. In a follow-up paper, we aim to explore some of the advantages of the prepolarization approach.

Introduction

NMR spectroscopy is limited by weak nuclear spin polarization levels, resulting in a poor signal-to-noise ratio (SNR). Thus, overcoming the Boltzmann polarization is a wide-spread concept, and many different techniques have already been developed. Notable techniques (Kovtunov et al., 2018; Eills et al., 2023) are dynamic nuclear polarization (DNP) (Ardenkjaer-Larsen et al., 2003) (Barker, 1962)(Abraham et al., 1959), parahydrogen-induced polarization (PHIP) (Bowers and Weitekamp, 1986)



(Bowers and Weitekamp, 1987), signal amplification by reversible exchange (SABRE) (Adams et al., 2009), Spin-Exchange
25 Optical Pumping (SEOP) (Happer et al., 1984) and brute-force hyperpolarization (Brewer and Kopp, 1976). All of these
techniques, except the brute-force method, have one thing in common: despite allowing for higher polarization levels (i.e. DNP
can result in up to 100% polarization), they are only applicable to specific samples or molecules, lack repeatability and are
unquantifiable. Another challenge is the complexity behind such methods. For example, DNP requires an additional microwave
source and a radical acting in the same space as the sample (in a low field setting for Overhauser DNP, see e.g. Kiss et al. (2016),
30 or in a high field setting for bullet dissolution DNP, see e.g. Kouřil et al. (2019)).

A brute-force hyperpolarization method achieved by raising the magnetic field intensity results in more modest enhance-
ments, but has the advantage of also being applicable to a larger range of samples without the use of additives. The prerequisites
are an external magnet providing sufficiently high fields (the prepolarizer), in which the sample can be polarized, and a rapid
yet adiabatic transfer to a lower-field spectrometer. The main challenges with this method are to reduce the size, acquisition
35 cost, and operating expense of the higher field magnet, and to establish an appropriate sample transfer procedure. The advent
of high- T_c superconducting wires has widened the operational window of field independence (hence avoiding magnet quench-
ing) to at least 40 T, and the introduction of pulsed tube coolers in the 1990's, which together have lowered the complexity
of operating cryogen-free cryostats. Furthermore, the world energy crisis has led to an increased installation volume of solar
and wind power in many regions, so that the renewable operation of cooled superconducting magnets at highest fields is now
40 within reach. We are therefore confident that this is an advantageous path to progress along, which we now consider in more
detail.

The Zeemann spin polarization decays exponentially in time with the spin-lattice relaxation constant T_1 , posing a further
limitation of this method in principle, so that fast adiabatic transfer is absolutely required. Secondly, T_1 also depends on the
polarizing magnetic field and rapidly decreases at very low fields. It is therefore important that the sample does not pass any
45 zero-field regimes (here a criterion of $|B| > 1$ mT is used). The time dependence of the total polarization is described by

$$P(t, B) = P_{t=0} + (P_{t=\infty} - P_{t=0}) \left[1 - \exp\left(-\frac{t}{T_1(B)}\right) \right], \quad (1)$$

and depicted in Figure 1 for a sample with $T_1 = 5$ s in a 5 T prepolarizer and a 1.4 T spectrometer setup (as relevant for the
experimental setup in this work) assuming that T_1 stays constant and the sample does not pass through any zero-field regimes
during transfer. For these fields, (5 T \rightarrow 10 mT \rightarrow 1.4 T), and a transfer time of 2 s and $T_1 = 5$ s, a maximum polarization
50 enhancement of about 2.6 is achievable.

Brute-force hyperpolarization has already been demonstrated at 2.3 K by (Hirsch et al., 2015) to achieve a 1600-fold en-
hancement in pyruvic acid. Here we want to show that brute-force works even at room temperature, to achieve enhanced
and hence useful polarization levels for benchtop NMR systems. We report experimental results on the enhancement for six
different samples, with 0.70 s $< T_1 < 5.18$ s, and ideal field configurations to preserve as much polarization as possible.

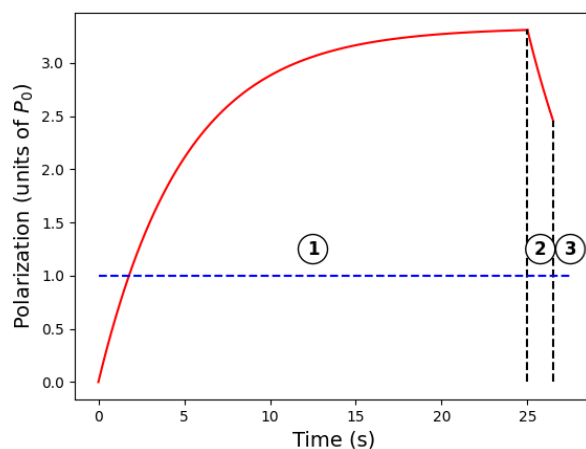


Figure 1. Estimation of the longitudinal polarization based on eq. (1), for a sample with $T_1 = 5$ s during the experiment. Here, the field-dependence of T_1 has been neglected to simplify the explanation. (1) The sample is placed for $5T_1$ in a 5 T prepolarizer to be fully polarized. (2) The sample loses some polarization during transfer due to T_1 relaxation. The transfer time is 2 s. (3) NMR signal acquisition is started right after insertion of the sample (rightmost dashed vertical line). The dashed blue horizontal line represents the 1.4 T spectrometer's Boltzmann polarization level P_0 . Dropping below this line would result in no enhancement.

55 Experimental Setup and Procedure

A 5 T cryogen-free Nb-Ti 2-coil superconducting magnet system with a 28 cm warm bore acts as prepolarizer and is used in combination with a Nanalysis 60 MHz benchtop NMR system. Six standard samples (see Table 1) with different values of T_1 are used for easy quantification of total polarization. The T_1 values have been determined using a straightforward inversion recovery sequence. The height of the spectrometer with respect to the equator of the prepolarizer was not optimized, so there was a slight offset.

Table 1. Samples used in the prepolarization experiments and their T_1 values at 1.4 T. They were determined using the inversion recovery method. CuSO_4 was used as a relaxation agent to decrease the T_1 of H_2O .

Sample	$\text{H}_2\text{O}/\text{D}_2\text{O}$ (1:1)	H_2O	Ethanol	0.5 mM CuSO_4 in H_2O	1 mM CuSO_4 in H_2O	2 mM CuSO_4 in H_2O
T_1 (s)	5.18	3.43	2.34	1.75	1.24	0.70

To determine the effects of prepolarization in different setups, five measurement series have been conducted; see Table 2. Here, d is defined as the horizontal separation between the 180 mm bore center of the prepolarizer and the spectrometer's 5 mm bore, and δB denotes the stray field of the prepolarizer or the Earth's magnetic field, respectively, inside the spectrometer



bore (measured with a Hall probe). The stray field of the NMR magnet itself is Halbach-shielded and vanishes outside the spectrometer.

Table 2. Five measurement series have been performed to investigate prepolarization for differing circumstances. Series (1) and (2) have a higher field during transfer and thus better T_1 , but worse homogeneity inside the spectrometer. Series (3) and (4) should have better homogeneity, but lower field (thus lower T_1) during transfer. Then, the prepolarizer was turned off to perform a reference series (5).

Series Number	Distance d (m)	Prepolarizer	Stray Field δB (mT)	Prepolarization Used?	Spectra Recorded
(1)	2	on	4	No	5
(2)	2	on	4	Yes	20
(3)	3	on	0.3	No	5
(4)	3	on	0.3	Yes	20
(5)	Reference	off	0.05	No	5

In our experiments, only 1H spectra were considered. Series (5) acts as reference series for signal strength and linewidth without perturbations through external magnetic fields. Series (1) and (3) are performed to determine the effects of the stray field on signal strength and linewidth. In these series, five spectra per sample were recorded and averaged. Lastly, series (2) and (4) were used to determine the effects of prepolarization. Here, twenty spectra per sample were recorded and averaged to estimate the uncertainty in the enhancement due to manual transfer. For the prepolarization, the samples were placed in the prepolarizer for about $5 \times T_1$ and manually transferred to the spectrometer within 1.5 s to 2 s (see Figs. 1 and 2). The spectra were recorded within the first second after transfer. A full shim of the spectrometer (27 active coils) was required before every series, because the prepolarizer stray field negatively affected the homogeneity inside the spectrometer. Series (1) and (2) had to be performed on the same shim to be comparable. The same held for series (3) and (4).

The total polarization was determined by integrating over the signal peak. The integration region was defined as $\Omega = \{\nu : I(\nu) > 0.05 \max\{I(\nu)\}\}$, such that regions with a signal strength less than 5% of $\max\{I(\nu)\}$ were dropped, see Figure 3. We chose this method to take line broadening into account, which depended only on the homogeneity of the magnetic field, and to count as many spins as possible. Taking the peak of the spectrum would not hold complete information about the total polarization. Additionally, we defined the enhancement ϵ as the ratio of polarization magnitudes with and without prepolarization as follows

$$\epsilon = \frac{\int_{\Omega} I_{PP}(\nu) d\nu}{\int_{\Omega} I_0(\nu) d\nu} \quad \text{with} \quad \Omega = \{\nu : I(\nu) > 0.05 \max\{I(\nu)\}\}. \quad (2)$$

Table 3. NMR acquisition parameters during each measurement.

Data Points	Flip Angle	Dwell Time	Receiver Gain	Num. Scans	Spectral Width	$T_2^*(2\text{ m})$	$T_2^*(3\text{ m})$	Transfer Time
2048	80.57°	1.36 ms	2	1	12 ppm	78 ms	157 ms	2 ± 0.5 s

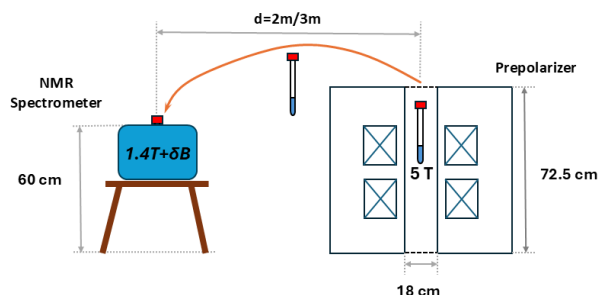


Figure 2. Sample transfer geometry (top) and procedure (bottom). The sample is manually transferred from the cryogen-free 5 T superconducting magnet on the right, to the permanent magnet benchtop 1.4 T NMR system on the left. Magnet separation and relative arrangement is crucial for maintaining a sufficiently strong polarizing stray field.

Results and Discussion

The results for the enhancement and the linewidth are given in Table 4. For better visualization, one representative $\text{H}_2\text{O}/\text{D}_2\text{O}$ spectrum for each column of Table 4 is selected and plotted in Figure 4.

Table 4. The experimental results represented by the enhancement ϵ and the linewidth Γ , eq. (2) (rows sorted by increasing T_1 -values). The enhancement is greater than 1 for the $\text{H}_2\text{O}/\text{D}_2\text{O}$, H_2O and ethanol samples. The enhancement is more pronounced at $d = 2$ m because of the larger field amplitude during transfer. As a tradeoff, the linewidth increases significantly. At $d = 3$ m the enhancement is more modest, but there are no losses in linewidth.

Sample	d (m)	Enhancement ϵ		Linewidth Γ (Hz)		
		2	3	2	3	Reference
$\text{H}_2\text{O}/\text{D}_2\text{O}$ (1:1)		2.62 ± 0.29	1.82 ± 0.08	7.56 ± 0.22	3.62 ± 0.09	4.08 ± 0.03
H_2O		1.52 ± 0.09	1.17 ± 0.04	8.07 ± 0.12	4.11 ± 0.08	4.14 ± 0.02
Ethanol		1.22 ± 0.10	1.08 ± 0.08	6.60 ± 0.15	4.30 ± 0.12	4.19 ± 0.01
0.5 mM CuSO_4 in H_2O		0.96 ± 0.05	1.00 ± 0.03	22.06 ± 0.06	3.37 ± 0.02	4.55 ± 0.01
1 mM CuSO_4 in H_2O		0.93 ± 0.03	1.04 ± 0.01	22.67 ± 0.10	3.53 ± 0.05	4.77 ± 0.02
2 mM CuSO_4 in H_2O		0.97 ± 0.02	1.04 ± 0.01	22.88 ± 0.02	4.10 ± 0.13	5.12 ± 0.01

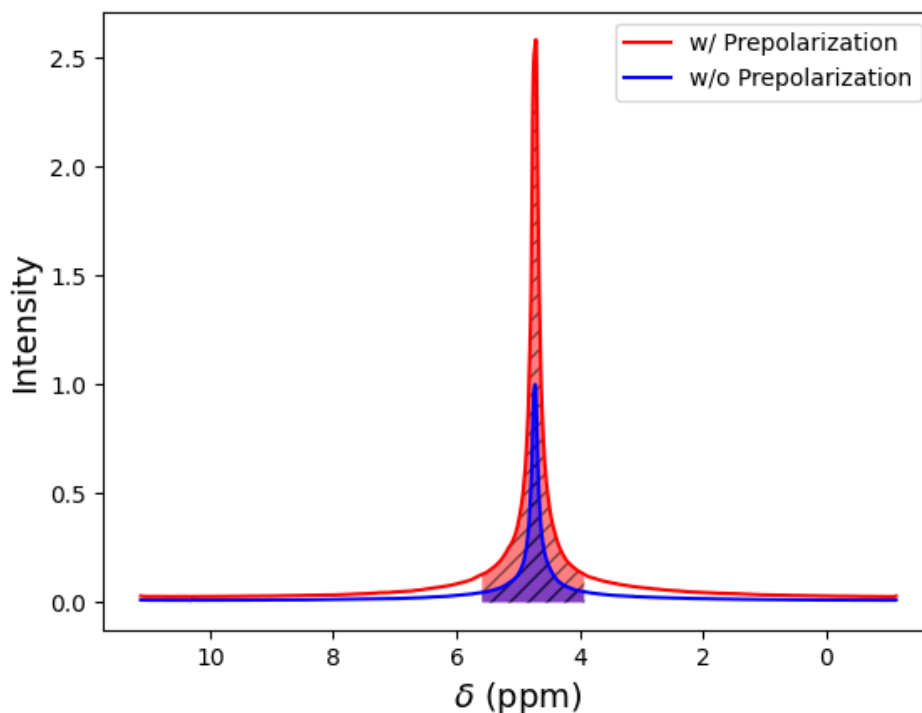


Figure 3. Normalized spectrum of the H₂O/D₂O sample with and without prepolarization at $d = 2$ m normalized. The spectrum with prepolarization shows a much larger peak. The equal range integration regions, used to characterize the total polarization and obtain the enhancement ϵ , is marked in red and blue.

85 The data (see Table 4 and Fig. 4) indicate a significant enhancement in polarization for the H₂O/D₂O, H₂O and ethanol samples, with enhancements of 2.62, 1.52, and 1.22 at $d = 2$ m (series (1) and (2)). At the same time, the linewidth increases, causing the spectrometer to lose resolution in chemical shift. At $d = 3$ m (series (3) and (4)), the enhancement is more modest for these samples, but still significant. Here, no increase in linewidth was observed. For the CuSO₄ solutions with low T_1 , no enhancement was observed. The larger magnetic field clearly has a positive effect on the enhancement, but also the drawback
 90 of increased linewidth. To extrapolate the data for T_1 times that were not covered by the data and obtain a phenomenological equation for the enhancement, it is treated as a function $\epsilon(T_1)$ with the boundary conditions $\epsilon(T_1 = 0) = 1$ and $\epsilon(T_1 \rightarrow \infty) = 5\text{ T}/1.4\text{ T} = 3.57$. Furthermore, it should grow exponentially for small T_1 , and converge exponentially for large T_1 due to equation 1. Thus, a hyperbolic tangent, Eq. 3, was chosen as fit function for $\epsilon(T_1)$. The exponential function in the argument of the tanh is introduced as a damping factor, to better describe the slower convergence for large T_1 .

95
$$f(T_1, a, b, c) = \frac{4.57}{2} + \frac{2.57}{2} \tanh[(a + e^{-bT_1})(T_1 - c)] \quad (3)$$

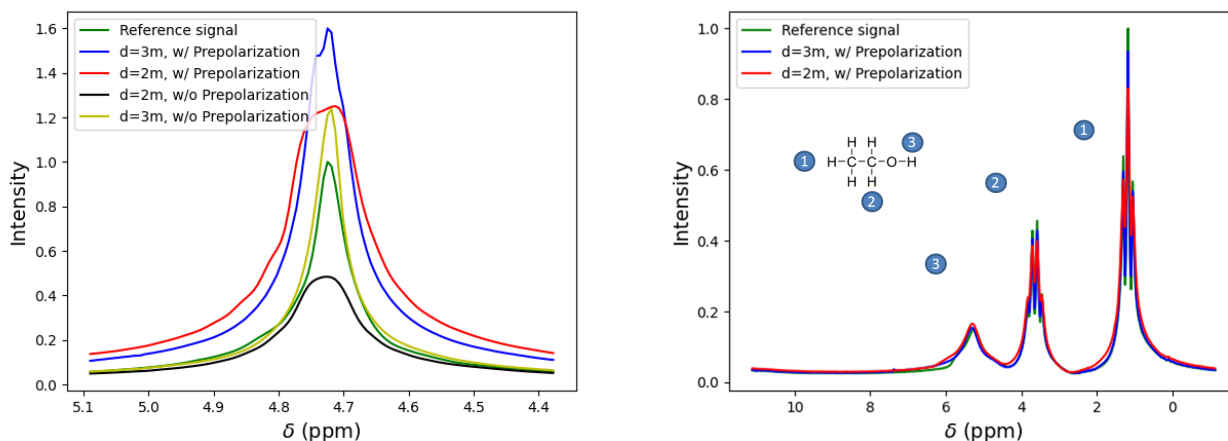


Figure 4. Left: One H₂O/D₂O spectrum of $d = 2\text{ m}/3\text{ m}$ and with/without prepolarization, as well as a reference signal with the prepolarizer turned off. The linewidth is increased for the 2 m measurements, accordingly the signal amplitude decreases. This is a field inhomogeneity effect and an active T_1 equilibration process. The total polarization can be obtained through integration and is shown in Table 4. Right: Prepolarization spectra of Ethanol at $d = 2\text{ m}/3\text{ m}$, as well as a reference spectrum. At a separation of $d = 2\text{ m}$, the increase in linewidth affects the chemical shift resolution so much, that two peaks almost become inseparable without significant increase in signal strength.

The fit resulted in values of $a = 0.6$, $b = 0.4$ and $c = 4.5$. When using an enhancement of $\epsilon \geq 1.1$ as criterion and our result for $\epsilon(T_1)$, it follows that $T_1 \geq 2.3\text{ s}$ can be estimated as threshold in our setup. Samples with even lower T_1 can benefit from prepolarization as well if the experimental setup is further optimized. Increasing the prepolarizer field strength ($> 10\text{ T}$), decreasing transfer times, or using stronger guiding fields can accomplish this.

100 Outlook: Toward HTS-based Prepolarizers

To reduce the impact of the prepolarizer's stray field on the spectrometer's field homogeneity, the spectrometer should be positioned in the equatorial plane of the prepolarizer center at a distance slightly greater than $d = 2\text{ m}$. Alternatively, the spectrometer can be placed directly below the prepolarizer. For either configuration, a stray field of at least $\delta B \simeq 1\text{ mT}$ is required in the spectrometer bore. This ensures that the stray field affects homogeneity of the spectrometer's magnetic field as little as possible, while still avoiding zero-crossings during sample transfer. To minimize the transfer time, the prepolarizer should be placed as close to the spectrometer as feasible. Most importantly, increasing the central magnetic field of the prepolarizer is

A promising approach to achieving higher fields is the use of compact high-field magnets based on high-temperature superconductors (HTS). The use of HTS at elevated temperatures reduces the need for complex and space-consuming cryogenic infrastructure. In particular, second-generation (2G) HTS tapes allow the prepolarizer to operate within the temperature range

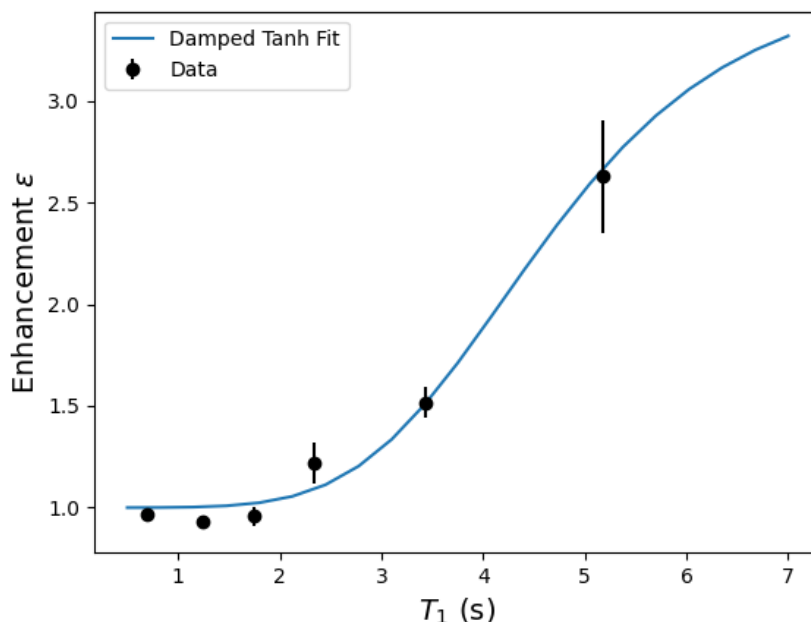


Figure 5. The enhancement behavior ($d = 2$ m, $n = 2048$ plotted over sample T_1) shows a plateau for values of T_1 lower than the total required transfer time, so the plateau corresponds to losing most polarization during transfer, and thus dropping below the Boltzmann level of the 1.4 T magnet. Since the sample cannot be fully re-polarized to the 1.4 T level by the NMR magnet before data acquisition, $\epsilon < 1$ is measured. For higher values of sample T_1 , more polarization is retained and hence measured as a stronger signal. The errors for the data points are given by the mean squared error over all 20 measurements.

of 20 K to 65 K, which is compatible with standard pulse-tube cryocoolers. The prospectively smaller size of HTS magnets also reduces the required transfer distance. In addition, appropriate magnetic-field configurations such as Halbach configurations, Maxwell- or Braunbek-architecture of coils (very well known in magnetic resonance imaging in healthcare), or the inclusion of shielding coils, can be used to reduce stray fields. To accommodate standard samples, a warm bore suitable for 5 mm NMR
115 tubes is essential. Presently, we are preparing a "simple", field-optimized 5 T design that uses a double pancake coil configuration as prepolarizer, with a height of about 5 cm (magnet only) that fulfills these requirements. It requires 36 meter of HTS-tape.

The potential of compact HTS technology has already been shown in the literature. Noteworthy are, e.g., the 45.5 T "Little Big Coil" by Hahn et al. (2019) with an outer diameter of 34 mm and a height of 54 mm for insertion into a 31 T bore; the
120 DUDA magnets first introduced by Arndt et al. (2021) with a bore of 8 mm, an outer diameter of 38 mm, and a stack height of 11.2 mm; as well as the high-field 23 T pocket magnet developed by Gao et al. (2024) with a bore of 8 mm, a diameter of 24 mm, and a height of 20 mm.

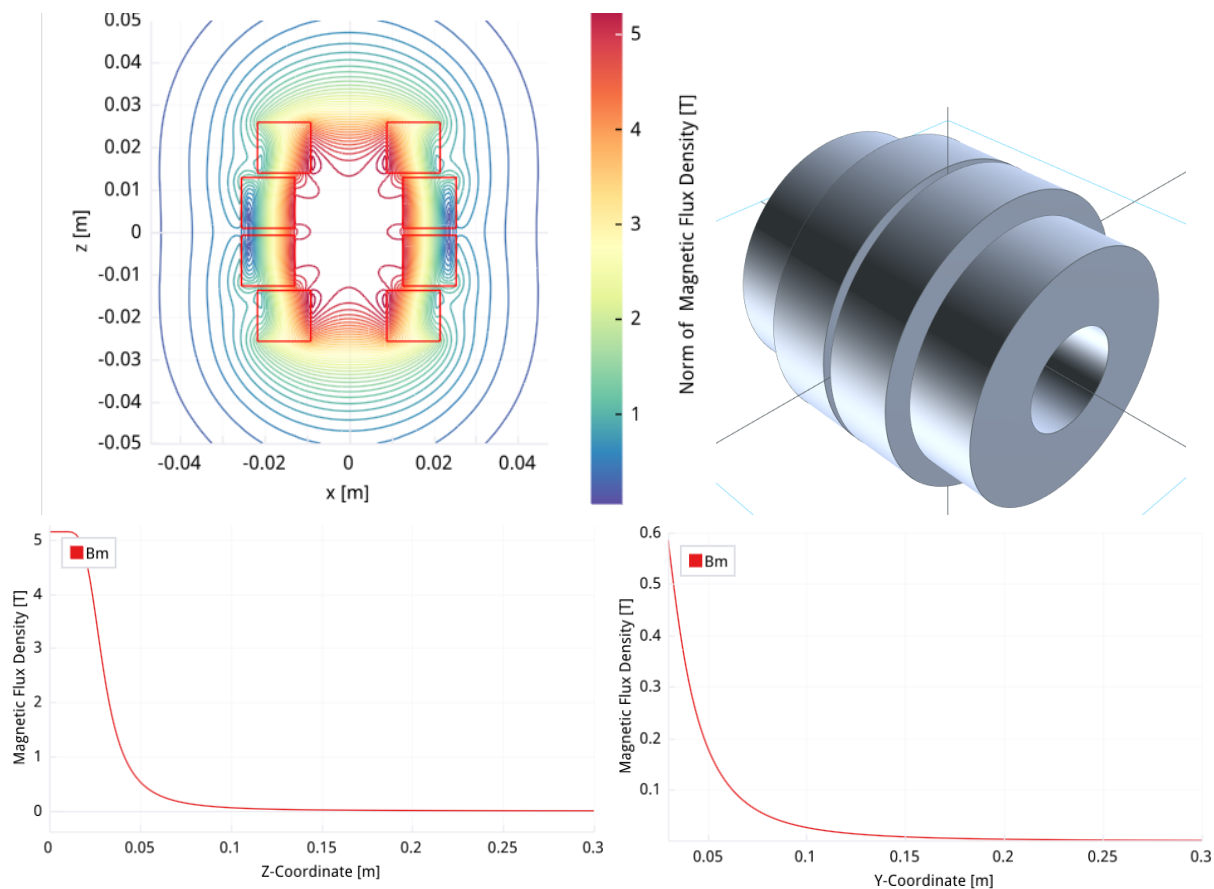


Figure 6. Magnetic field profile of prepolarizer/ micro NMR magnet according design number 2 (top left), general outline (top right), field profile along the z-axis (bottom left) and stray field in the radial direction (bottom right). RAT-GUI was used to create the graphics and perform the simulations..

Conclusion

We demonstrated the convenience and efficiency of brute-force hyperpolarization in increasing the polarization and resulting SNR in compact benchtop NMR spectrometers by a factor of around 2.8. The transport method between the magnets was performed manually and hence not optimized. Improving it would further preserve polarization, for example using a shielded tunnel and a bullet transfer method (Kouřil et al., 2019), a robotic system (Yang, J. and Xin, R. and Lehmkuhl, S. and Korvink, J. G. and Brandner, J., 2024) or compressed air (Villanueva-Garibay et al., 2025). Due to the simplicity of the method and the moderate requirements for samples with T_1 sufficiently large, it is applicable to liquid-state chemical systems and will significantly improve NMR results in widespread small spectrometer installations. Especially heteronuclei can profit from this method due to their low γ . We further project the use of dry 2G-HTS magnets that can access fields as high as 40 T, as a powerful option to implement compact high-field prepolarizers in combination with strategies for appropriate stray fields.



Acknowledgments

The research was funded by the Deutsche Forschungsgemeinschaft within CRC 1527 HyPERiON. We acknowledge the support
135 of Markus Breig for providing the laboratory photographs, as well as Anna Leismann for support in preparing the NMR
samples.

Author contributions. TA, BH, and JK conceptualized the research topic. PJ planned and performed all the experiments and evaluated the
data. SL took responsibility for the NMR samples, trained PJ and interns on NMR techniques and sample preparation, and supervised the
analysis. MD was involved in magnet engineering. JH and MB discussed the data and results. PJ and JK prepared the first draft. All authors
140 contributed to the manuscript and prepared the final version.

Competing interests. JGK is a shareholder of Voxalytic GmbH, a company that develops magnetic resonance systems. JGK is also a member
of the editorial board of Magnetic Resonance. The other authors declare that there are no competing interests.



References

- Abraham, M., McCausland, M. A. H., and Robinson, F. N. H.: Dynamic Nuclear Polarization, *Phys. Rev. Lett.*, 2, 449–451, 145 <https://doi.org/10.1103/PhysRevLett.2.449>, 1959.
- Adams, R. W., Aguilar, J. A., Atkinson, K. D., Cowley, M. J., Elliott, P. I., Duckett, S. B., Green, G. G., Khazal, I. G., López-Serrano, J., and Williamson, D. C.: Reversible interactions with para-hydrogen enhance NMR sensitivity by polarization transfer, *Science*, 323, 1708–1711, 2009.
- Ardenkjaer-Larsen, J. H., Fridlund, B., Gram, A., Hansson, G., Hansson, L., Lerche, M. H., Servin, R., Thaning, M., and Golman, K.: 150 Increase in signal-to-noise ratio of > 10,000 times in liquid-state NMR, *Proc Natl Acad Sci USA*, 100(18), 10 158–63, 2003.
- Arndt, T., Holzapfel, B., Noe, M., Nast, R., Hornung, F., Kläser, M., and Kudymow, A.: New coil configurations with 2G-HTS and benefits for applications, *Superconductor Science and Technology*, 34, 2021.
- Barker, W. A.: Dynamic Nuclear Polarization, *Rev. Mod. Phys.*, 34, 173–185, <https://doi.org/10.1103/RevModPhys.34.173>, 1962.
- Bowers, C. R. and Weitekamp, D. P.: Transformation of Symmetrization Order to Nuclear-Spin Magnetization by Chemical Reaction and 155 Nuclear Magnetic Resonance, *Phys. Rev. Lett.*, 57, 2645–2648, <https://doi.org/10.1103/PhysRevLett.57.2645>, 1986.
- Bowers, C. R. and Weitekamp, D. P.: Parahydrogen and synthesis allow dramatically enhanced nuclear alignment, *Journal of the American Chemical Society*, 109, 5541–5542, <https://doi.org/10.1021/ja00252a049>, 1987.
- Brewer, W. and Kopp, M.: Brute-force nuclear orientation, *Hyperfine Interactions*, 2, 299–305, 1976.
- Eills, J., Budker, D., Cavagnero, S., Chekmenev, E. Y., Elliott, S. J., Jannin, S., Lesage, A., Matysik, J., Meersmann, T., Prisner, T., et al.: 160 Spin hyperpolarization in modern magnetic resonance, *Chemical reviews*, 123, 1417–1551, 2023.
- Gao, C., Chen, P.-H., Alaniva, N., Björgvinsdóttir, S., Pagonakis, I., Däpp, A., Urban, M., Gunzenhauser, R., and Barnes, A.: 23 Tesla high temperature superconducting pocket magnet, *Superconductor Science and Technology*, 37, 2024.
- Hahn, S., Kim, K., Kim, K., Hu, X., Painter, T., Dixon, I., Kim, S., Bhattarai, K. R., Noguchi, S., Jaroszynski, J., and Larbalestier, D. C.: 45.5-tesla direct-current magnetic field generated with a high-temperature superconducting magnet, *Research Letter*, 570, 496–499, 2019.
- 165 Happer, W., Miron, E., Schaefer, S., Schreiber, D., van Wijngaarden, W. A., and Zeng, X.: Polarization of the nuclear spins of noble-gas atoms by spin exchange with optically pumped alkali-metal atoms, *Phys. Rev. A*, 29, 3092–3110, <https://doi.org/10.1103/PhysRevA.29.3092>, 1984.
- Hirsch, M. L., Kalechofsky, N., Belzer, A., Rosay, M., and Kempf, J. G.: Brute-Force Hyperpolarization for NMR and MRI, *Journal of the American Chemical Society*, 137, 8428–8434, 2015.
- 170 Kiss, S., Rostas, A., Heidinger, L., Spengler, N., Meissner, M., MacKinnon, N., Schleicher, E., Weber, S., and Korvink, J.: A microwave resonator integrated on a polymer microfluidic chip, *Journal of Magnetic Resonance*, 270, <https://doi.org/10.1016/j.jmr.2016.07.008>, 2016.
- Kouřil, K., Kouřilová, H., Bartram, S., Levitt, M. H., and Meier, B.: Scalable dissolution-dynamic nuclear polarization with rapid transfer of a polarized solid, *Nature Communications*, 10, 2019.
- Kovtunov, K. V., Pokochueva, E. V., Salnikov, O. G., Cousin, S. F., Kurzbach, D., Vuichoud, B., Jannin, S., Chekmenev, E. Y., Goodson, 175 B. M., Barskiy, D. A., et al.: Hyperpolarized NMR spectroscopy: d-DNP, PHIP, and SABRE techniques, *Chemistry—An Asian Journal*, 13, 1857–1871, 2018.
- RAT-GUI: <https://www.rat-gui.com/index.html>, software.



- 180 Villanueva-Garibay, J. A., Tilch, A., Alva, A. P. A., Bouvignies, G., Engelke, F., Ferrage, F., Glémot, A., le Paige, U. B., Licciardi, G., Luchinat, C., Parigi, G., Pelupessy, P., Ravera, E., Ruda, A., Siemons, L., Stenström, O., and Tyburn, J.-M.: A fast sample shuttle to couple high and low magnetic fields. Applications to high-resolution relaxometry, *Magnetic Resonance Discussions*, 2025.
- Yang, J. and Xin, R. and Lehmkuhl, S. and Korvink, J. G. and Brandner, J.: Development of a fully automated workstation for conducting routine SABRE hyperpolarization., *Scientific Reports*, 14, 21 022, <https://doi.org/10.1038/s41598-024-71354-x>, 2024.